Journal of Materials Science and Nanotechnology
Volume 12 | Issue 1
ISSN: 2348-9812

Research Article Open Access

Characterizations of $Cu_2FeSnSe_4$ Thin Films Synthesized from Nanoparticles Powder

Hadjer Rekkache[1], Louardi Yandjah[1, 2, *], Lakhdar Bechiri[1], Noureddine Benslim[1], Safia Alleg[3] and Xavier Portier[4]

[1]LESIMS - LEAM, Département de Physique, Faculté des Sciences, Université-Badji Mokhtar, Annaba, Algeria
[2]Department of Material Sciences, Faculty of Science and Technology, Univ-Souk-Ahras 41000
[3]Laboratoire de Magnétisme et Spectroscopie des Solides (LM2S), Département de Physique, Faculté des Sciences, Université-Badji Mokhtar, Annaba, Algeria
[4]CIMAP, Centre de recherche sur les ions, les matériaux et la photonique, CEA, UMR 6252 CNRS, ENSICAEN, Normandie Université, 6-Boulevard du Maréchal Juin, Caen Cedex 14050, France

[*]**Corresponding Author**: Louardi Yandjah, Department of Material Sciences, Faculty of Science and Technology, Univ--Souk-Ahras 41000, Algeria, Tel: +213662613309, E-mail: louardi.yandjah@gmail.com

Citation: Hadjer Rekkache, Louardi Yandjah, Lakhdar Bechiri, Noureddine Benslim, Safia Alleg et al. (2024) Characterizations of Cu2FeSnSe4 Thin Films Synthesized from Nanoparticles Powder, J Mater Sci Nanotech nol 12(1): 102

Received Date: March 22, 2024 **Accepted Date:** April 22, 2024 **Published Date:** April 27, 2024

Abstract

$Cu_2FeSnSe_4$ (CFTSe) thin film were synthesized on glass substrate by thermal evaporation method at T_s=400° C, starting from elemental powders mixed by a mechanical alloying process. The structural, morphological, compositional, optical and electrical properties of CFTSe semiconductor have been investigated by X-ray diffraction (XRD), Raman spectroscopy, scanning electron microscopy (SEM), transmission electron microscopy (TEM), energy dispersive X-ray analysis (EDAX), spectroscopic ellipsometry (SE) and Van Der Pauw technique, respectively. The morphology and chemical composition of the (CFTSe) microparticles have been confirmed by the scanning electron microscope (SEM) and energy dispersive spectrometer (EDS). XRD results showed that the film has a polycrystalline nature with cubic structure and a lattice parameter α =5.682 Å with a texture along the (111) plane. The optical constants and dielectric parameters were found between 1.00 to 5.00 eV, the optical absorption coefficient (α) was above 6.5×103 cm^{-1} and the band gap were found at E_g = 1.60 eV. The thin film presented a hole density of 1.646×10^9 (cm^{-3}), a hole mobility of $2.709x10^2$(cm^2 V^{-1} s^{-1} and an electrical conductivity of 7.146×10^2 ($\Omega^{-1}.cm^{-1}$).

Keywords: $Cu_2FeSnSe_4$; Mechanical Alloying; Nanoparticles; Thin Films; Thermal Evaporation; Semiconductor Cubic Structure

Introduction

Stannite-group minerals have attracted substantial research interest due to their potential application in solar cells, thermoelectric, optoelectronics and energy storage. Cu_2FeSnS_4 (CFTS) and $Cu_2FeSnSe_4$ (CFTSe) are considered to be amongst the better solar cell materials; they contain earth abundant elements with high absorption coefficient and have good stabilities.

The scarcity of natural energy sources combined with the polluting conventional energy production make the scientific community looking for alternative sustainable energy sources. In this context, the search for new materials and methods in photovoltaic by production of thin films with low cost has been stimulated [1]. Different types of semiconductor materials have received great interest especially Se-based absorbers due to their relative abundance at reasonable cost and their attractive optoelectronic properties, such as CISe, CIGSe, CTSe and CZTSe [2]. More recently, some researchers were interested in studying quaternary semiconductors such as CFTSe and CZTSe because they are characterized by their interesting range gap, inexpensive, non-toxic and having high absorption coefficients [3]. In solar cell technology, CFTSe is considered a promising alternative to conventional materials like silicon and cadmium telluride. The material's optimal bandgap (around 1.0-1.2 eV) allows it to absorb a broad spectrum of sunlight, enhancing its efficiency in converting solar energy into electricity. In the field of thermoelectrics, CFTSe exhibits potential for waste heat recovery and power generation applications. A good thermoelectric material should have a high Seebeck coefficient, low thermal conductivity, and high electrical conductivity.

In addition, thin films of $Cu_2FeSnSe_4$ can be synthesized using various methods, including physical vapor deposition (PVD) techniques such as co-evaporation or sequential deposition [4], selenization of RF magnetron sputtered precursors [1], reaction time of selenization [5], a simple solvothermal method [6], chemical spray pyrolysis [7].

In this present work, we present a complete study focused on a $Cu_2FeSnSe_4$ thin film grown by thermal evaporation whose advantages are its efficiency, simplicity, low cost, weak impact on the physical properties of the target material and allowing a good control of the film thickness with a nanometer size accuracy [8]. (CFTSe) thin film was prepared by thermal evaporation process offers advantages such as simplicity and compatibility with various substrate materials. However, it may have limitations regarding uniformity and control over stoichiometry in complex compound systems like $Cu_2FeSnSe_4$. The optimization of process parameters is necessary to achieve desired film properties. The composition, structure, morphology and electro-optical proprieties of CFTSe thin film were studied. The results suggest that $Cu_2FeSnSe_4$ semiconductors are promising candidates for solar cells.

In summary, the synthesis and characterization of $Cu_2FeSnSe_4$ thin films play a crucial role in advancing solar cell technology, thermoelectric, and other relevant fields by optimizing material properties, improving device performance, and expanding the range of potential applications. These efforts contribute to the development of sustainable energy solutions and innovative technologies with broad societal and economic impacts.

Experimental Details

In the experimental section of the study, crucial parameters such as deposition rate during thermal evaporation, annealing conditions, and the purity of starting materials play significant roles in determining the properties of the synthesized $Cu_2FeSnSe_4$ (CFTSe) thin films.

Materials Synthesis

$Cu_2FeSnSe_4$ thin film was synthesized by a simple step process. Copper, Iron, Tin and Selenium as pure starting components (Cu, Fe and Sn granular, 99.99%, from Balzers) and (Se pellets, 99.99%, from Balzers) were weighted to reach the following molar proportion of Cu: Fe: Sn: Se/2:1:1:4 and they were milled using high energy planetary ball mill (Fritsch premium line P-7) [9]. The powder/balls weight ratio was 1/2 with a rotational speed of 300 rpm and a milling time of 3 hours and 30 minutes. The resulting

nano powder was employed to produce $Cu_2FeSnSe_4$ thin film were grown by thermal evaporation onto pre-cleaned glass substrates and on (100)-oriented Si wafers doped with $10^{15}/cm^3$ of boron substrates; This technique as described in detail elsewhere [10] under vacuum at about 10^{-6} Torr and the substrates temperature was fixed at T_s=400°C. The deposition rate measured by a quartz crystal microbalance for thin film deposition was 150 Å/s for thermal evaporation.

Characterizations

Structural properties of the powders and the films were investigated by X-ray diffraction (XRD) using Philips Xpert NPD Pro diffractometer equipped with a Cu-Kα radiation λ=1.54187 Å, in the range of *2θ* between 10° and 100° with a step size value of 0.02° and a counting time of 2s. Furthermore, to identify the possible secondary phases in the fabricated films, Raman spectroscopy was performed using a Spectro Raman system equipped with a confocal Horiba Jobin-Yvon T64000 spectrometer and a laser source of excitation wavelength λ=632.8 *nm*. Characterization techniques assist in optimizing synthesis parameters thereby enhancing material performance and stability for various applications. The synthesis and characterization of CFTSe thin films are crucial for advancing solar cell technology, thermoelectric and other fields, promoting efficient and sustainable energy conversion.

The characterization of surface morphology was performed by scanning electron microscopy (SEM) and the chemical composition was determined by energy dispersive X-ray spectrometry (EDAX) installed in a JEOL6400 SEM microscope (JEOL Ltd, Tokyo, Japan). Transmission electron microscopy (TEM) was used to investigate the microstructure of the samples and the microscope employed was a 2010 FEG JEOL microscope operated at 200 keV.

The optical properties of the CFTSe thin films were analyzed by spectroscopic ellipsometry (SE) using a phase modulation ellipsometer. The data were collected while the incident light was scanned between 1.5 eV and 5.0 eV with steps of 0.02 eV at the incident angle of 66.2°. This was carried out by means of a Jobin–Yvon Ellipsometer (UVISEL). Hall concentration, Hall mobility and the resistivity measurements were determined at room temperature by the Van Der Pauw technique.

Results and Discussion

Powder Sample

A typical X-ray diffraction (XRD) pattern of the $Cu_2FeSnSe_4$ nano powder is shown in Figure1. The observed peaks with high intensities corresponding to (111), (220), and (311) planes at values of angles 2θ=27.18°, 45.15°, 53.51° and lower intensities at (400), (331), (422), and (511) planes with *2θ* values of 65.61°, 72.56°, 83.26° and 89.68°, respectively indicate that CFTSe has a cubic structure with a lattice parameter a=5.682Å which is consistent with the standard pattern of $Cu_2FeSnSe_4$ (PDF file #27-0167). This result is in good agreement with previous works on this material according to [11]. However, we notice a very small peak at $2\theta = 30.71^{\circ}$ corresponding to an interreticular distance (*d*=2.90 Å), which originates from a ternary phase Cu_2SnSe_3 (PDF file #89-2879) meaning that this phase is in a very small quantity in the powder.

The morphology of the CFTSe milled powder is illustrated by an SEM view presented in Figure2.a with a large cluster (up to 200 μm diameter) of agglomerated grains, the inset in the top right-hand side is an enlargement of the corresponding image centered on one of these clusters. The compositional analysis of the obtained from EDS spectroscopy is Cu: 28.01 at. %, Fe: 5.13 at. %, Sn: 13.18 at. % and Se: 53.68 at.%. Obviously, our sample is iron and tin-lacking due to the mechanical alloying process (see Figure2.b).

The crystallite size of CFTSe powder was estimated from the most intense (111) and (220) peaks to be 24.74 nm using Debye Scherer's formula [12,13]:

$$D = \frac{k\lambda}{\beta_{hkl} \cos \theta_{hkl}} \quad (1)$$

Where D is the average crystallite size, k is the shape factor (k=0.9), λ is the X-ray diffraction wavelength (λ=1.54187Å) and β_{hkl} is the full width at half maximum (FWHM) of the corresponding peak position in radian.

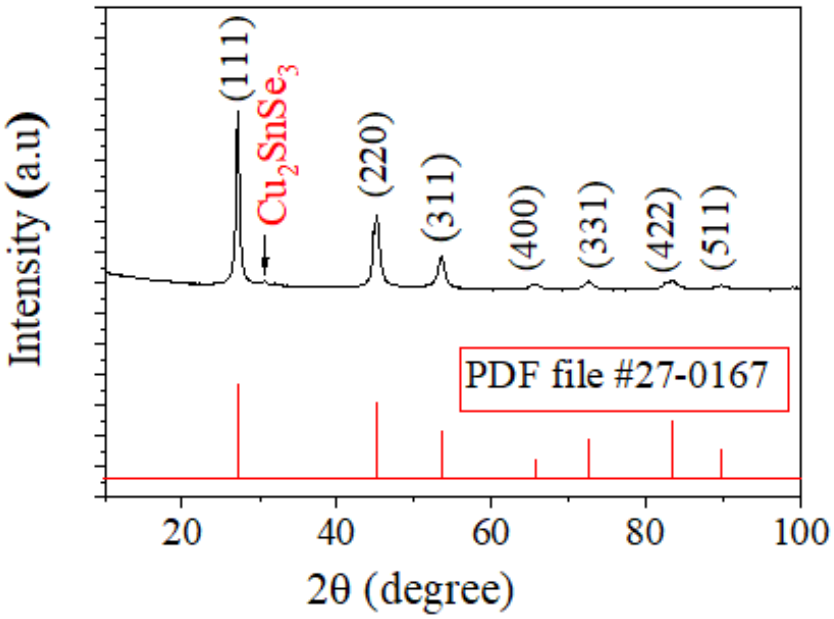

Figure 1: XRD pattern of the $Cu_2FeSnSe_4$ nanopowder

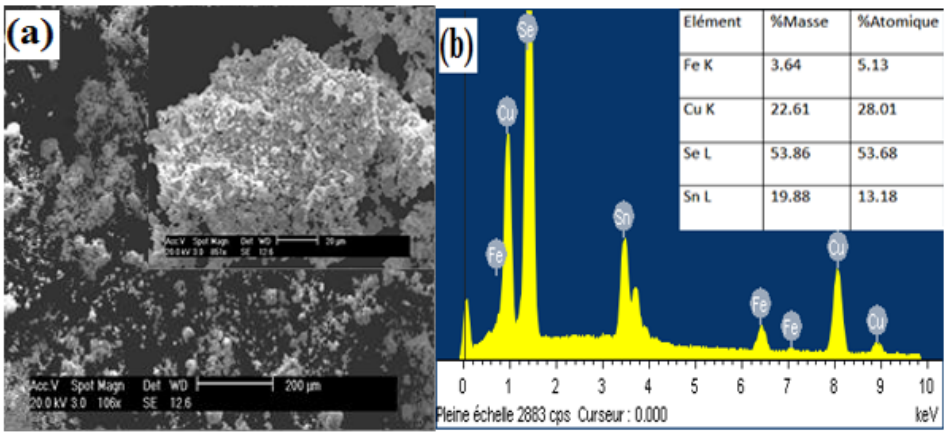

Figure 2: (a) SEM image of CFTSe powder, (b) Corresponding EDS spectrum.

In order to determine the value of the dislocation density *(δ)*, we used Williamson and Smallman's formula [14]:

$$\delta = \frac{1}{D^2} \quad (2)$$

The estimated value of the dislocation density for the deposited powder was found to be

$$\delta = 1.63 \times 10^{15} lines/m^2.$$

Moreover, for a better characterization, the crystallite size (D) and the lattice strain (ε) induced in the CFTSe powder were calculated using the Williamson's and Hall's formula equation as indicated below [15]:

$$\beta_{hkl} \cos\theta_{hkl} = \frac{k\lambda}{D} + 4\varepsilon \sin\theta_{hkl} \quad (3)$$

The Scherrer's formula for crystallite size and the micro strain terms are both included in the Hall-Williamson equation.

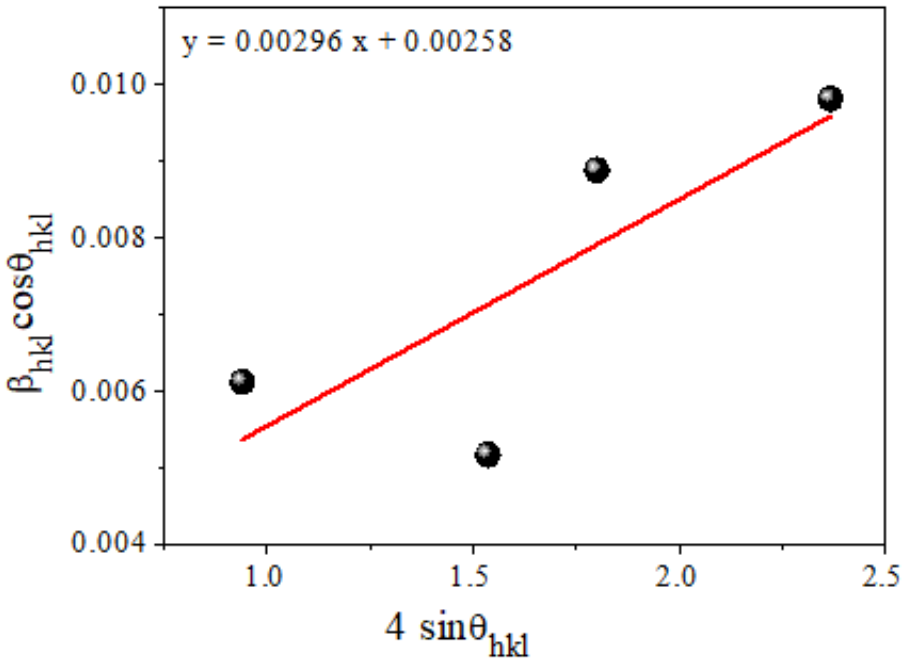

Figure 3: The Williamson-Hall analysis of the CFTSe powder

Figure3. shows that (D) and (ε) can be calculated from the slope and y-axis intercept of $\beta_{hkl}\cos\theta_{hkl}$ versus 4sin θ_{hkl} plots, respectively. The values are given in Table 1. The positive residual strain value for the $Cu_2FeSnSe_4$ nanoparticles indicates that it is the extension strain.

Table 1: Structural parameters values of the $Cu_2FeSnSe_4$ milled powder

Milling time (min)	lattice parameter (Å)	Crystallite size (D) by Scherrer method (nm)	$\delta\ (10^{15})$ lines / m^2	Williamson's and Hall's method
				D(nm) $\varepsilon\ (10^{-3})$
210	5.68	24.74	1.63	53.78 2.96

The crystal structure of the CFTSe powder was also analyzed by means of TEM observations. A selected area electron diffraction (SAED) shown in Figure4. (a) confirms the presence of the crystalline CFTSe phase with the distinct planes corresponding to the (111), (220), (311), (400), (331), (422) and (511) planes of a cubic structure having a lattice parameter value of 0.568 nm which are in good agreement with the XRD data. Interestingly, the two circled diffraction points correspond to iron (Fe). Figure4. (b) shows a typical dark field TEM image and brings the evidence of the crystalline nature of the grains. A high-resolution transmission electron microscope (HREM) image of the CFTSe powder is shown in Figure4. (c) from which one can measure an interplanar spacing d= 0.207 nm. This value is in good agreement with the (111) d spacing of the iron cubic structure (d_{011}= 0.207 nm). At last, the corresponding Fast Fourier transform (FFT, Figure4. (d)) of the HREM image confirms the cubic structure of the grain since it is consistent with a [1,1,0] projection.

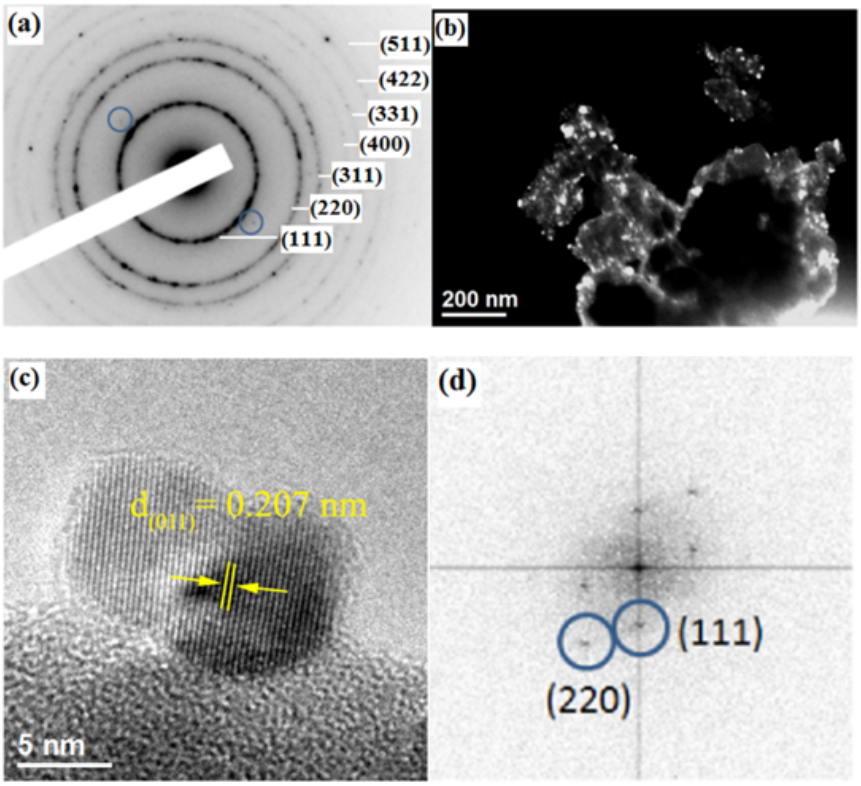

Figure 4: (a) The corresponding selected-area electron diffraction (SAED) pattern. (b) Dark-field transmission electron microscopy image. (c) HREM image of two small grains and (d) The corresponding Fast Fourier transform of the HREM image confirming the presence of Fe grains.

$Cu_2FeSnSe_4$ Thin Film

$Cu_2FeSnSe_4$ thin films were synthesized by thermal evaporation technique on a glass substrate temperature and at T_s=400°C. Figure5. shows the X-ray diffraction (XRD) pattern of the CFTSe film. It can be seen that the sample is composed of three phases. Firstly, a quaternary cubic phase whose XRD peaks are located at 2θ =26.61°, 44.04°, 56.45°,61.85°, 75.65°, 90.02°, and corresponding to interplanar *d* spacing 3.35Å, 2.05Å, 1.63Å, 1.50Å, 1.26Å, 1.09Å, respectively.

These peaks are identified from reflections of (111), (220), (311), (400), (331), (511), which was compared with the interplanar *d* spacing of $Cu_2FeSnSe_4$ (PDF file #27-0167). Secondly, Cu_2SnSe_3 ternary cubic phase with peaks at 2θ =31.23°, 33.16°, 66.55°, 66.20°, corresponding to 2.87Å, 2.70Å, 1.41Å, 1.35Å distances, respectively and they are identified from reflections of 200, 220, 400, 331 lattice planes, which are in good agreement with the PDF file #89-2879. Finally, binary phases are observed such as SnSe at 2θ =25.46°, 29.58°, 30.57°, 37.80°, 47.79°, 49.89°, 52.23°, 54.60°, 91.08° and Cu_2Se at 2θ =13.09°, 25.38°, 52.18°. They correspond well with PDF files #32-1382, #35-1042 and PDF file #19-0401, respectively.

In this work the Full Width at Half Maximum (FWHM) of the 111, 220,and (311) peaks in the CFTSe thin film. The FWHM values obtained were 2θ =31.23°, 33.16°and 66.55°, respectively. These values indicate that the as-synthesized thin film possesses excellent crystallinity. Moreover, the average grain size was calculated to be 24 nm using the Scherrer equation.

The Raman spectra analysis provides valuable information not only about the structure of the CFTSe thin film but also about the presence of other compounds such as Cu_2SnSe_3, Cu_xSe, and $SnSe_2$ within the synthesized CFTSe. This is because the most intense X-ray diffraction (XRD) peaks of these compounds coincide with those of CFTSe. Raman spectra not only can describe the structure of CFTSe thin film but also can detect the presence of Cu_2SnSe_3, Cu_xSe and $SnSe_2$ in the synthesized CFTSe as the most intensive XRD peaks of these compounds coincide with those of CFTSe.

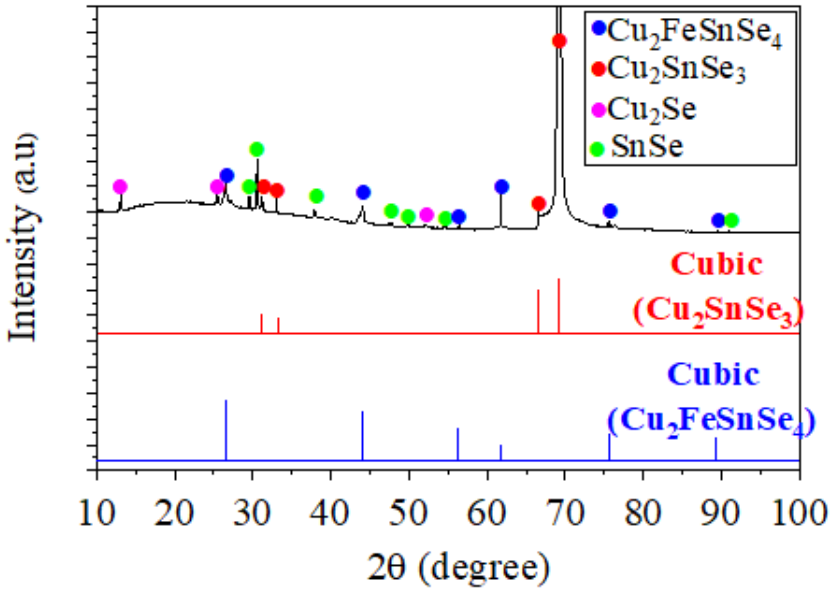

Figure 5: XRD pattern of the $Cu_2FeSnSe_4$ thin film

In addition, Raman scattering analysis was used as a complementary tool of XRD data to confirm the presence of different phases present in the film. As demonstrated by Figure6, five main peaks were found at 58 cm^{-1}, 67cm^{-1}, and 228 cm^{-1} and they can be attributed to Cu_2SnSe_3 [16]; 106 cm^{-1}, 175 cm^{-1} can be assigned to SnSe and $FeSe_2$ phases [7,4], respectively (see Figure6. below).

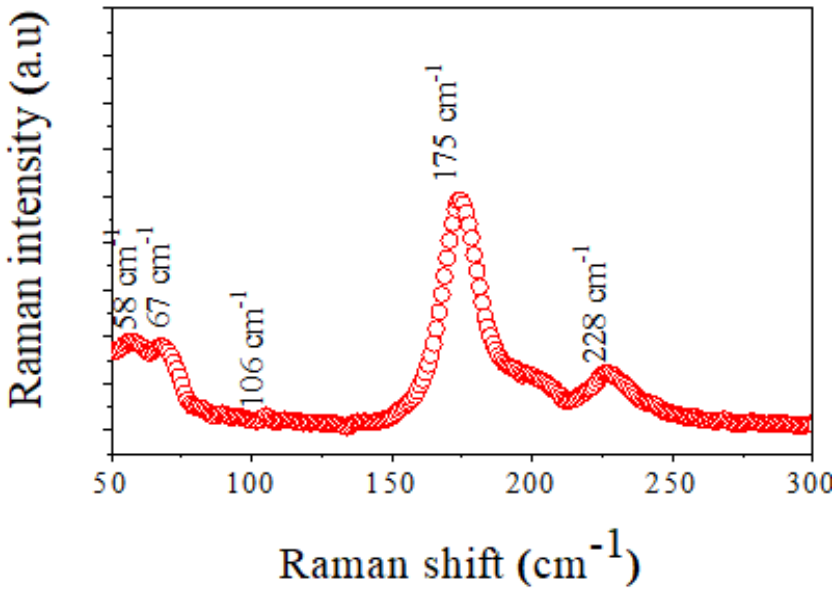

Figure 6: Raman spectrum of the $Cu_2FeSnSe_4$thin film

Figure7.a shows is an SEM image of a cross sectional view of the film. It provides an idea of the surface morphology of the film whose average thickness is about 950 nm. The inset shown at the top right-hand side is a top view of the film with a lower magnification. The crystallite size is well visible and it shows small spherical grains. ImageJ software (see histogram below in Figure7.b) statistic confirmed the average grain size. This value is represented by the peak position of the Gaussian curve of the histogram x_c =0.2 μm.The surface of CFTSe thin film is Dense and no voids. Some information on grain sizes and crystallinity of the sample can be directly got by means of SEM. Notably, the SEM analysis reveals a grain size of approximately 200 nm, which is larger than the value calculated using the Scherrer equation. This finding is consistent with the observations made by Salome et al. [17], who also reported similar differences in their research.

In addition, Figure7.c presents an EDX spectrum of the CFTSe deposited film. The average chemical composition ratio is Cu: 59.53at. %, Fe: 0.98 at. %, Sn: 3.94at. % and Se: 35.54 at.%. This quantitative analysis is the result of various measurements from different regions on the $Cu_2FeSnSe_4$ film surface. Evidently, we can notice that the Cu-rich composition (i.e., Cu / (Fe+Sn+Se>1) of our sample is not close to the expected stoichiometry of 2:1:1:4.

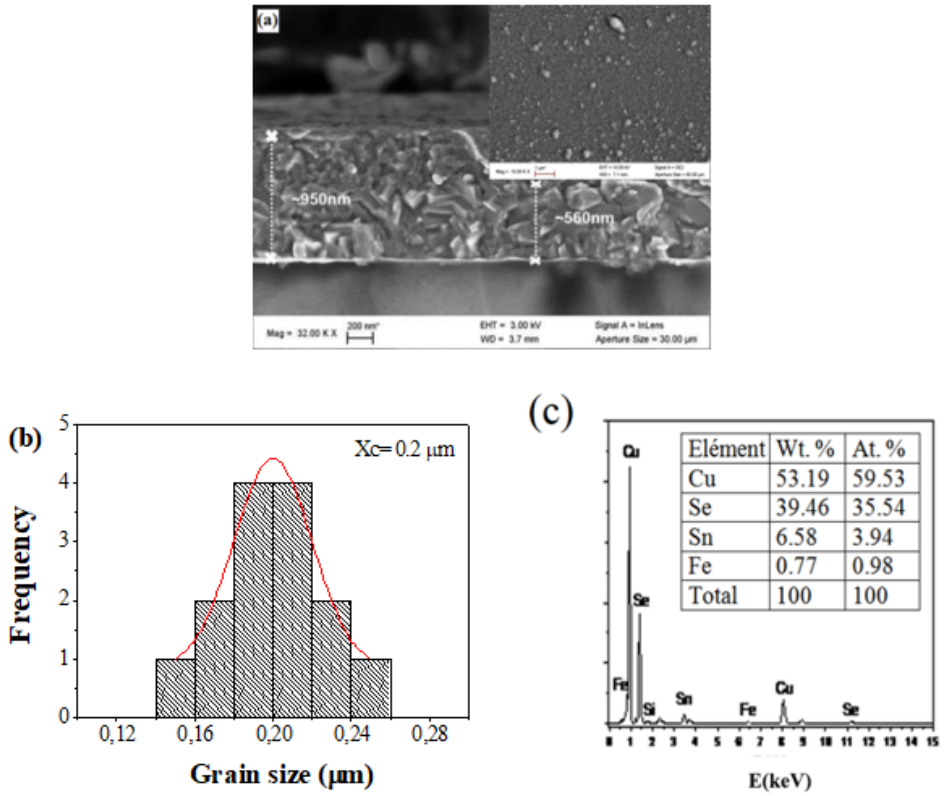

Elément	Wt. %	At. %
Cu	53.19	59.53
Se	39.46	35.54
Sn	6.58	3.94
Fe	0.77	0.98
Total	100	100

Figure 7: (a) Cross sectional SEM image of the CFTSe thin film, (b) The particle size distributions, (c) EDX spectrum from the CFTSe thin film

Optical Properties

The SE spectra consist in the measurement of ψ and Δ ellipsometric angles defined from the fundamental equation of ellipsometry [18]:

$$\frac{r_p}{r_s} = \rho = tan\psi e^{i\Delta} \quad (4)$$

Where ρ is the complex ratio of r_p and r_s, r_p and r_s being the complex reflection coefficients for parallel and perpendicular polarizations of the light, respectively. The measurement can be performed as a function of wavelength and angle of incidence.

Optical constants of interest, namely, the refractive index (*n*), extinction coefficient (*k*) as function of photon energy (eV) (see Figure8) and the thickness of CFTSe deposited film on (100) oriented silicon substrate was analyzed by spectroscopic ellipsometry (SE) technique using phase modulation ellipsometer. This method is extremely accurate and does not request a reference material.

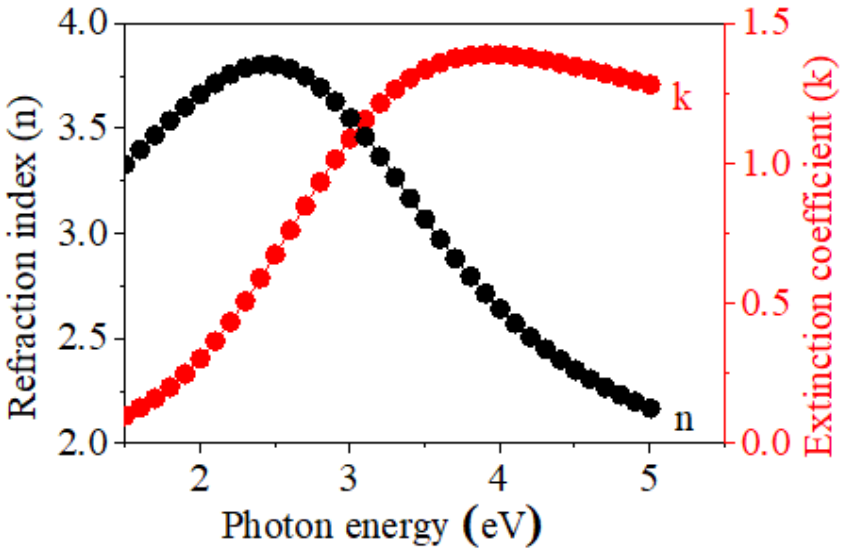

Figure 8: Spectral dependence of refractive index (*n*) and extinction coefficient (*k*) for the obtained CFTSe film deposited on Si (100)

The optical response to incident photon energy is represented by a complex dielectric function denoted by: $\varepsilon=\varepsilon_1+i\varepsilon_2$

Dielectric parameters (ε_1, ε_2), the real part and the imaginary part respectively, were evaluated using Eq (5), (6) below [19].

$$\varepsilon_1 = n^2 + k^2 \quad (5)$$

$$\varepsilon_2 = 2nk \quad (6)$$

The real part of the dielectric constant indicates how much the material will slow down the speed of light, while the imaginary portion describes how a dielectric material absorbs energy from an electric field due to dipole motion. The results are shown in Figure9.a:

The absorption coefficient ($\alpha\sim 6.5\times10^3 cm^{-1}$) and normal-incidence reflectivity (R) for CFTSe films see Figure9.b were defined as follows [20, 21], respectively:

$$\alpha = \frac{4\pi k}{\lambda} \quad (7)$$

$$R = \frac{(n-1)^2 + k^2}{(n+1)^2 + k^2} \quad (8)$$

Where (*k*) is the extinction coefficient, (λ) is the wavelength and (*n*) is the refraction index.

The large absorption coefficient of CFTSe makes these materials very suitable as absorber materials in thin-film solar cells, and is in accord with the conditions of the solar cell absorption layer [22,23,24].

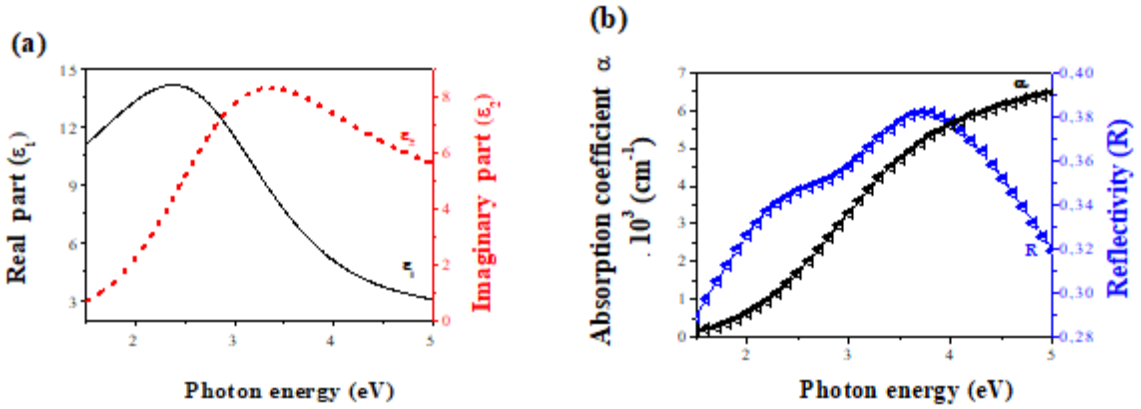

Figure 9: (a) Real (ε_1) and imaginary (ε_2) parts of the dielectric spectra and (b) Plot of the absorption coefficient (α) and normal-incidence reflectivity (R) with respect to photon energy for the CFTSe film

The values of *n, k,* ε_1, ε_2, R and α are in good agreement with data reported elsewhere [25,26], but the difference remains in the maximum and minimum values. This variation most likely results from the preparation process or from the presence of iron in the film. Additionally, the optical conductivity was obtained using Eq (9) below [27]:

$$\sigma = \frac{\alpha n c}{4\pi} \quad (9)$$

Where σ is the optical conductance, c is the velocity of the radiation in the space, n is the refractive index and α, the absorption coefficient. The variation of the optical conductance with the incident photon energy of CFTSe film is illustrated in Figure 10 where, the highest value is ≈3.65×108cm^{-1}.

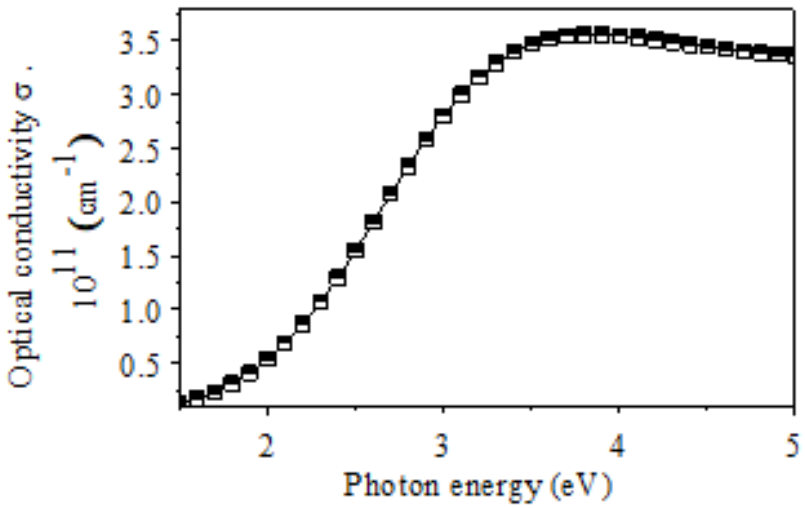

Figure 10: Optical conductivity values (σ) versus incident photon energy for the CFTSe thin film

The energy gap of the $Cu_2FeSnSe_4$ thin film was studied using Tauc's relation presented by [28]:

$$\alpha h\nu = A(h\nu - E_g)^n \quad (10)$$

Where A is a constant, *α* the absorption coefficient, (*hν*) the photon energy and E_g the optical band gap energy. The value of n is 1/2 for direct transition and 2 for indirect transition [28].

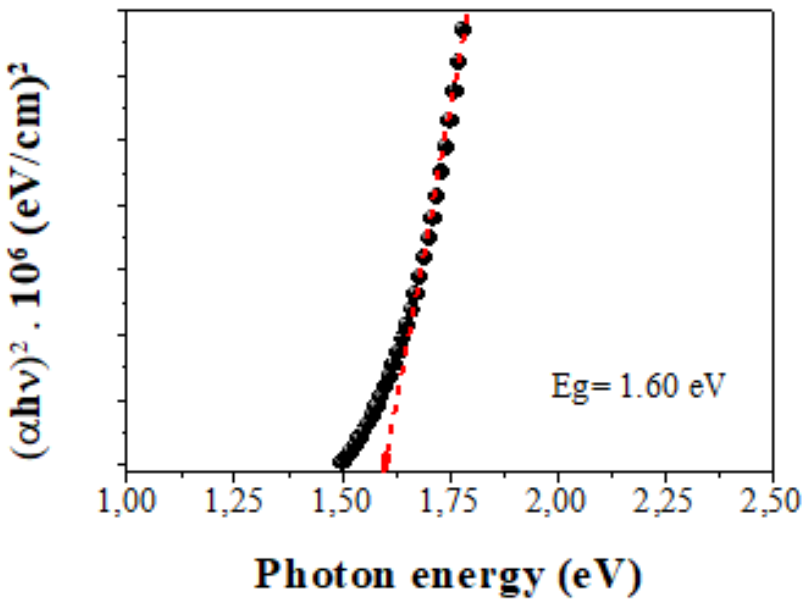

Figure 11: Plot of αhν2versus hν (eV) for the CFTSe thin film

Figure 11 shows the plot of $(\alpha h\nu)^2$ versus *hν* and the optical bandgap of the CFTSe film can be analyzed by linear extrapolation of the line to the energy axis and the optical band gap value is found to be E_g =1.60 *eV* [29].

At last, electrical properties for the CFTSe thin film were analyzed. Hall concentration, Hall mobility and electrical conductivity were determined at room temperature by the Van Der Pauw technique and have been found to be $1.646x10^{19}$ (cm^{-3}), $2.709x10^{2}$ ($cm^{2}\ V^{-1}s^{-1}$) and $7.146x10^{2}$ ($\Omega^{-1}.cm^{-1}$), respectively. These electrical measurements confirmed the p-type nature of the film.

Conclusion

The main contributions of the study involve the successful synthesis and characterization of $Cu_2FeSnSe_4$ (CFTS) thin films using a mechanical alloying process and thermal evaporation technique. Structural analyses reveal that the CFTS powder consists of crystallites with an average size of 24.74 nm and a cubic structure, with a lattice parameter a = 5.682 Å. A small amount of the (Cu_2SnSe_3) ternary phase was also observed. The crystallite size was estimated using both Debye Scherer's and Williamson–Hall methods.

CFTS thin film was prepared at a substrate temperature of 400°C, resulting in the formation of quaternary $Cu_2FeSnSe_4$, ternary (Cu_2SnSe_3), and binary (SnSe, $FeSe_2$) phases. X-ray diffraction studies confirmed the cubic structure with a (111) texture, while Raman spectra supported this behavior and revealed persistent modes of the various phases.

Optical properties of the CFTS semiconductor show a high absorption coefficient (α~ 6.5×103cm-1) and an optical band gap of Eg=1.60 eV.

This study investigates the synthesis and characterization of CFTS thin films, examining phase formation and optical properties. The findings contribute to the development of efficient and sustainable energy conversion solutions, establishing CFTS as a promising material for optoelectronic applications.

References

1. Meng, H Deng, JH Liping Zhu, L Sun, P Yang, et al. (2014) Synthesis of Cu2FeSnSe4 thin film by selenization of RF magnetron sputtered, Materials Letters, 117: 1-3.

2. R Pallavolu, AN Banerjee, VR Minnam Reddy, SW Joo, H Rani Barai, et al. (2020) "Status review on the Cu2SnSe3 (CTSe) thin films for photovoltaic applications." Solar Energy, 208: 1001-30.

3. Meng, H Cao, H Deng, W Zhou, J Zhang, et al. (2015) Structural, optical and electrical properties of Cu2FeSnSe4 and Cu (In, Al) Se2 thin films, Materials Science in Semiconductor Processing, 39: 243-50.

4. B Khadka, JH Kim (2015) Structural, optical and electrical properties of Cu2FeSnX4 (X = S, Se) thin films prepared by chemical spray pyrolysis. Journal of Alloys and Compounds 638: 103-8.

5. Meng, H Deng, J Zhang, W Zhou, J Tao, et al. (2015) Structural and optical tunability by reaction time of selenization in Cu2FeSnSe4 thin films. Journal of Alloys and Compounds, 646: 68-72.

6. Zhang, M Cao, L Li, Y Sun, Y Shen, et al. (2013) Facile synthesis of Cu2FeSnSe4 sheets with a simple solvothermal method Materials Letters, 93: 111-4.

7. Hayashi, T Minemoto, G Zoppi, I Forbes, K Tanakaa, et al. (2009) Effect of composition gradient in Cu (In, Al) Se2 solar cells Solar Energy Materials and Solar Cells, 93: 922-5.

8. Özkartal, DT Noori (2021) Effects of thermal annealing on the characterization of p-NiO/n-GaAs heterojunctions produced by thermal evaporation. J Mater Sci: Mater Electron, 32: 13462-71.

9. Sehli, M Benabdeslem, N Benslim, L Bechiri, H Ayed, et al. (2014) Formation and Study of the Nanostructured CuAl0.5-Ga0.5Te2 Synthesized by Mechanical Alloying Processing JOM, 66: 985-91.

10. Rekkache, H Kassentini, L Bechiri, N Benslim, A Amara, et al. (2022) Study of Copper Tin Selenide Nanoparticles of Milled Powder and Thin Films, Journal of Nano Research, 72: 67-79.

11. Liu, M Hao, J Yang, L Jiang, C Yan, et al. (2014) Colloidal synthesis of Cu2FeSnSe4 nanocrystals for solar energy conversion. Materials Letters, 136: 306-9.

12. Chihi, B Bessais (2016) Synthesis and characterization of Cu2SnSe3 thin films by electrodeposition route. Superlattices and Microstructures, 97: 287-97.

13. S Sindhu, SR Maidur, PS Patil, BV Rajendra (2020) Influence of structure and surface morphology on optical limiting property of spray pyrolyzed ZCO thin films. Chemical Physics Letters, 759: 137975.

14. Astam (2016) Structural and optical characterization of Cu2SnSe3 thin films prepared by SILAR method, Thin Solid Films, 615: 324-8.

15. G Haji abadi, M Zamanian, D Souri (2019) Williamson-Hall analysis in evaluation of lattice strain and the density of lattice dislocation for nanometer scaled ZnSe and ZnSe: Cu particles, Ceramics International, 45: 14084-9.

16. Rincón, G Marcano, R Casanova, GE Delgado, G Marín, et al. (2015) Optical absorption, Raman spectra, and electrical properties of Mn-doped Cu2SnSe3 semiconductor compound. Physica Status Solidi (b), 253: 697-704.

17. MP Salomé, PA Fernandes, AF da Cunha (2010) Influence of selenization pressure on the growth of Cu2ZnSnSe4 films from stacked metallic layers. Phys Status Solidi (C), 7 : 913-6.

18. A Woollam, BD Johs, CM Herzinger, JN Hilfiker, RA Synowicki, et al. (1999) "Overview of variable-angle spectroscopic ellipsometry (VASE): I. Basic theory and typical applications", Proc. SPIE 10294, Optical Metrology: A Critical Review, 1029402: 1-26.

19. Kompa, U Chaitra, D Kekuda, M Rao K (2021) Investigation on structural, optical and electrical properties of Nd doped titania films and application of optical model- Materials Science in Semiconductor Processing, 121: 105293.

20. Ziti, B Hartiti, H Labrim, S Fadili, HJ Tchognia Nkuissi, et al. (2019) Effect of copper concentration on physical properties of CZTS thin films deposited by dip-coating technique, Applied Physics A, 125: 218.

21. Isik, N Gasanly (2016) Ellipsometric study of optical properties of GaSxSe1-x layered mixed crystals Optical Materials, 54: 155-9.

22. J Zhou, D Mei, XG Kong, XH Xu, LD Feng, et al. (2012) One-step synthesis of Cu (In,Ga)Se2 absorber layers by magnetron sputtering from a single quaternary target, Thin Solid Films, 520: 6068-74.

23. H Shi, Z Q Li, D W Zhang, Q Q Liu, Z Sun et al. (2010) Fabrication of Cu(In, Ga)Se2 thin films by sputtering from a single quaternary chalcogenide target. Progress in Photovoltaics: Research and Applications, 19: 160-4.

24. Walsh, SY Chen, SH Wei, XG Gong (2012) Adv Energy Mater, 2: 400-9. Kesterite thin-film solar cells: Advances in materials modelling of Cu2ZnSnS4. Advanced Energy Materials, 2: 400-409.

25. Gurieva, S Levcenko, S Schorr, M León, R Serna, et al. (2013) Characterization of Cu2SnSe3 by spectroscopic ellipsometry. Thin Solid Films, 535: 384-6.

26. G Choi, J Kang1, J Li, H Haneef, NJ Podraza, et al. (2015) Optical function spectra and bandgap energy of Cu2SnSe3.Applied Physics Letters, 106: 043902.

27. Usman, JO Dennis, AY Ahmed, KC Seong, YW Fen, et al. (2020) Structural characterization and optical constants of p-toluene sulfonic acid doped polyaniline and its composites of chitosan and reduced graphene-oxide, Journal of Materials Research and Technology, 9: 2238-7854.

28. R Pallavolu, RR Nallapureddy, HR Barai, SW Joo (2020) Effect of selenization temperature on the physical properties of Cu2SnSe3 thin films. Thin Solid Films, 709: 138238.

29. L iu, M Hao, J Yang, L Jiang, C Yan, et al. (2014) Colloidal synthesis of Cu2FeSnSe4 nanocrystals for solar energy conversion. Materials Letters, 136: 306-9.